PHYSICAL REVIEW B VOLUME 19, NUMBER 4 15 FEBRUARY 1979

# Structural interpretation of the vibrational spectra of $a$-Si:H alloys

G. Lucovsky, R. J. Nemanich, and J. C. Knights
*Xerox Palo Alto Research Center, 3333 Coyote Hill Road, Palo Alto, California 94304*
(Received 21 August 1978)

The ir and Raman spectra of $a$-Si:H alloys produced by plasma decomposition of $SiH_4$ are studied for a wide range of deposition conditions. The vibrational spectra display modes which can be characterized as predominantly hydrogen motions. Analysis of these modes shows four types of local Si-H bonding environments which are identified as SiH, $SiH_2$, $SiH_3$, and coupled $SiH_2$ or $(SiH_2)_n$ units. On the basis of these identifications, it is found that samples produced on high-temperature (above 200°C) substrates have SiH, $SiH_2$, and $(SiH_2)_n$ groups with very little $SiH_3$. In contrast, the ir and Raman spectra of samples produced on room-temperature or cooled substrates are dominated by vibrational modes of $SiH_3$ and $(SiH_2)_n$. The relative concentrations of these hydrogen-containing groups are not simply proportional to the total hydrogen concentration in a given sample.

## INTRODUCTION

This paper addresses the question of the local bonding environments of H in $a$-Si and $a$-Si:H alloys. The interest in a detailed understanding of these environments stems from changes in the electronic properties of $a$-Si brought about by the incorporation of hydrogen. It has been demonstrated that hydrogen incorporation at the level of $\sim 10^{19}/cm^3$ into sputtered $a$-Si reduces the number of defect sites controlling the conduction and recombination processes.[1] Similarly, if hydrogen is removed from plasma-deposited material, the defect density undergoes a dramatic increase that can be reversed by rehydrogenation.[2] However, above a certain level, brought about by changes in the deposition conditions, the excess hydrogen in plasma-deposited materials appears to be associated with an increase in the defect density.[3] The questions then arise as to whether there is more than one local bonding configuration for hydrogen, and if so, whether different bonding configurations play different roles with regard to the defect sites.

The first question has already been addressed by vibrational spectroscopy.[4,5] There have been several recent studies of the ir absorption and Raman scattering of $a$-Si:H alloys prepared by either plasma decomposition of $SiH_4$,[4-6] or by reactive sputtering in hydrogen.[4,7] Analysis of these results allows an identification of the spectral signatures for sites containing one H atom, SiH, or more than one H atom, $SiH_2$ and/or $SiH_3$. Specifically, the SiH environments are characterized by a bond-stretching mode at 2000 $cm^{-1}$ and a bond-bending mode at 630 $cm^{-1}$, whereas sites with more than one H atom exhibit additional features in a bond-bending frequency regime, 800–950 $cm^{-1}$, as well as new bond-stretching modes between 2050 and 2150 $cm^{-1}$. The complexity of these additional features is illustrated in the papers of Brodsky, Cardona, and Cuomo[4] (BCC) and Knights, Lucovsky, and Nemanich[5] (KLN). For example, in KLN the authors identify a weak feature at 860 $cm^{-1}$ in samples containing a well-resolved doublet with components at 845 and 890 $cm^{-1}$. Similarly, BCC note shifts as large as 15–20 $cm^{-1}$ in each of these doublet components. There has, however, been disagreement between BCC and KLN on the precise local environments responsible for the bond-bending modes. This difference in interpretation assumed larger significance when a correlation was established between electronically active defects and one of the modes in question at 845 $cm^{-1}$.[3] In an attempt to resolve this difference, we have undertaken a more detailed study of the vibrational spectra.

In this paper we present new spectra for $a$-Si:H alloys produced by plasma deposition from $SiH_4$. Using the dilution of $SiH_4$ in argon as a variable, we have been able to change the material structure so as to permit the resolution of the bending modes into two distinct doublets. From correlations between the stretching modes and these doublets we demonstrate that both the BCC and KLN models are operative, but in different deposition regimes. Specifically, we show that samples produced on high-temperature substrates, $T_S > 200$ °C, display features that can be attributed to both SiH and $SiH_2$ groups; these include a bond-bending doublet at 845 and 890 $cm^{-1}$ and a bond-stretching mode at 2090 $cm^{-1}$ which are due to the $SiH_2$ groups. Samples produced on room-temperature and cooled substrates can, depending on the relative dilution of the $SiH_4$ with Ar, yield spectra with features attributable to $SiH_2$ and/or $SiH_3$


©1979 The American Physical Society

groups. The $SiH_3$ groups are characterized by a *different* bond-bending doublet with components at 862 $cm^{-1}$ and 907 $cm^{-1}$ and a relatively sharp bond-stretching mode at 2140 $cm^{-1}$.

## EXPERIMENTAL DATA AND RESULTS

The samples reported in this study were produced by the plasma decomposition of $SiH_4$. The construction of the apparatus, as well as the variation of the deposition rate as a function of the deposition parameters, is discussed elsewhere.[8,9] For purposes of this presentation, the most important deposition parameter is the substrate temperature. However, as we will demonstrate, significant changes in the nature of the H incorporation can be achieved at a fixed substrate temperature by varying the power into the reactor, the electrical bias on the substrate, and the relative concentration of $SiH_4$ (as diluted by Ar).[9] Our primary interest is not in the relationship between deposition parameters and the resulting local order. Rather, we use the changes in the spectra due to variations in the deposition process to establish correlations between different modes in order to identify their structural origin. The ir measurements were made on a Perkin-Elmer Model 180 Spectrophotometer. The samples used in these transmission measurements were deposited onto high-resistivity Si substrates. The measurements were made using a double-beam mode of operation in which a Si substrate was used in the reference channel. The Raman measurements were made using 5309-Å excitation from a krypton-ion gas laser. The resultant spectra were analyzed with a Spex triple monochromator.

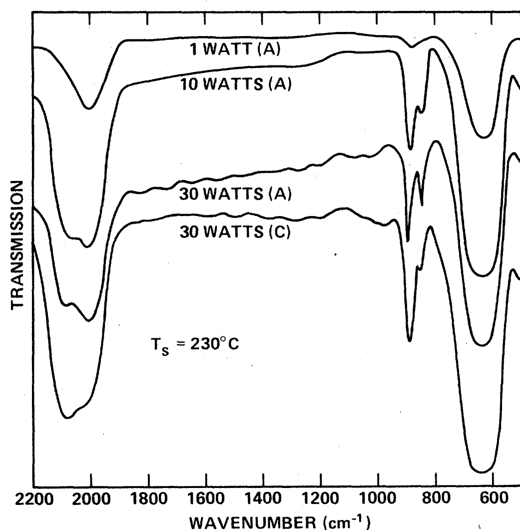


FIG. 1. ir transmission of a-Si:H for $T_s$ = 230 °C. (A) indicates a sample produced on an anode substrate and (C) indicates a sample produced on a cathode substrate.

The ir-absorption spectra shown in Fig. 1 are for a fixed substrate temperature of 230 °C, a fixed dilution of $SiH_4$ by Ar, 5 at.%, but with varying rf power and bias. Consider first the anode sample produced at the lowest rf power, 1 W; this spectrum is dominated by two strong absorption bands, one at 2000 $cm^{-1}$ and the second at 630 $cm^{-1}$. There is also very weak absorption evident at approximately 875 $cm^{-1}$. Increasing the rf power, as indicated in the 10- and 30-W samples, produces important changes in the ir-absorption spectra. There is an additional absorption band at about 2090 $cm^{-1}$, as well as significantly stronger absorption in the 850–900-$cm^{-1}$ regime. This latter absorption consists of a doublet with a relatively broad and strong component at approximately 890 $cm^{-1}$ and a sharper, but weaker component at 845 $cm^{-1}$. For samples produced on the anode, the absorption at 845 $cm^{-1}$ increases dramatically as the rf power is increased, growing more rapidly than either the absorption at 2090 or 890 $cm^{-1}$. In contrast, samples produced on the cathode show an even more pronounced growth of the 2090 and 890 $cm^{-1}$ modes with increasing rf power, but substantially weaker absorption and also less change with rf power in the 845-$cm^{-1}$ feature. As is evident here and in the study of Tsai *et al.*,[6] the differences in the character of the ir absorption as a function of rf power and bias are not simply the result of changes in the amount of H incorporated in the films. The H content in the 1-W sample is approximately 9 at.%, and rises to about 15 at.% in the 10-W sample. The concentration drops to about 13 at.% in the 30-W anode sample, and is just in excess of 15 at.% in the 30-W cathode sample.

The absorption constant $\alpha$ is plotted as a function of the rf power for the anode samples in Fig. 2. The absorption bands at 845 $cm^{-1}$ and 890 $cm^{-1}$ are sufficiently well resolved so that the peak absorption constant provides a good measure of the integrated absorption strength. In contrast, the absorption in the bond-stretching regime clearly has at least two contributions which are not as well resolved. However, no attempt was made to deconvolve this absorption into two bands using idealized line shapes, e.g., Gaussian or Lorentzian bands. It is evident that the absorption at 2000 $cm^{-1}$ is not due to the same group as that at 845, 890, and 2090 $cm^{-1}$. To identify the relationships between the latter three absorptions, we have plotted in Fig. 3 values of the relative absorption constants, $\alpha(890\ cm^{-1})/\alpha(2090\ cm^{-1})$ and $\alpha(845\ cm^{-1})/\alpha(890\ cm^{-1})$.[9] The nearly constant value of $\alpha(890\ cm^{-1})/\alpha(2090\ cm^{-1})$ establishes that these two vibrations are associated with one structural group. We will later assign these to an

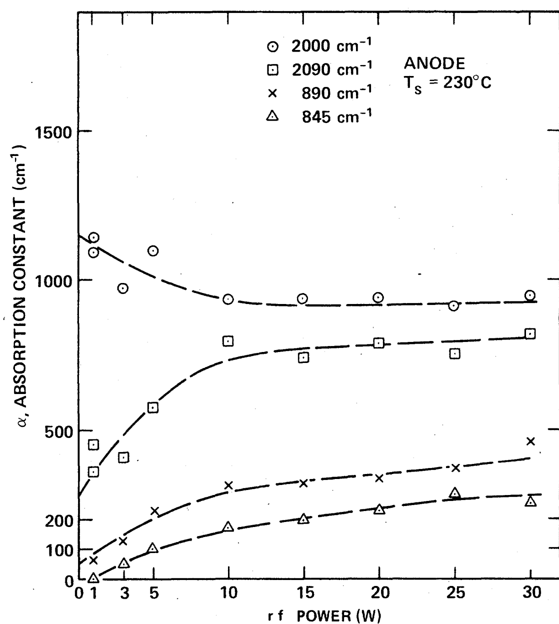


FIG. 2. Absorption constants of $a$-Si:H as a function of rf power for anode samples with $T_s = 230\,^\circ\mathrm{C}$.

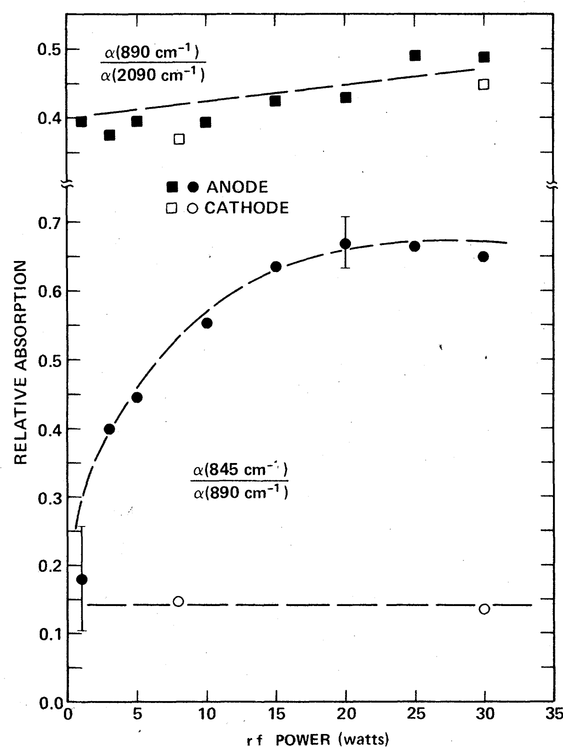


FIG. 3. Relative absorption as a function of rf power for $a$-Si:H for $T_s = 230\,^\circ\mathrm{C}$.

$SiH_2$ unit. The small increase in this ratio with increasing rf power may be associated with the fact that a deconvolution of the two bond-stretching vibrations was not attempted. The ratio $\alpha$(845 cm cm$^{-1}$)/$\alpha$(890 cm$^{-1}$) is very different for the anode and cathode samples. The constancy of the ratio for the cathode samples implies that the 845-cm$^{-1}$ absorption is also associated with the same structural group as the bands at 890 and 2090 cm$^{-1}$, $SiH_2$. The change in the ratio with increasing power for anode samples will be shown to be related to a coupling between neighboring $SiH_2$ groups into short chain segments of the form $(SiH_2)_n$. Similar changes in the relative absorptions can also be accomplished by varying the substrate temperature but maintaining a fixed rf power. This is illustrated in Fig. 4.

The absorption spectra for anode films deposited on room-temperature substrates are displayed in Fig. 5. These spectra show the ir absorption in the bond-stretching (1900–2200 cm$^{-1}$) and bond-bending (800–900 cm$^{-1}$) regimes, but do not include the bond-rocking regime near 650 cm$^{-1}$ since all of the spectra show similar strong and broad absorption in this region. For these films the rf power was fixed, but the dilution of $SiH_4$ with Ar was varied. The H content of the films was determined by a gas-effusion technique and decreases with increasing dilution of $SiH_4$. These spectra indicate two sets of doublets in the 800–

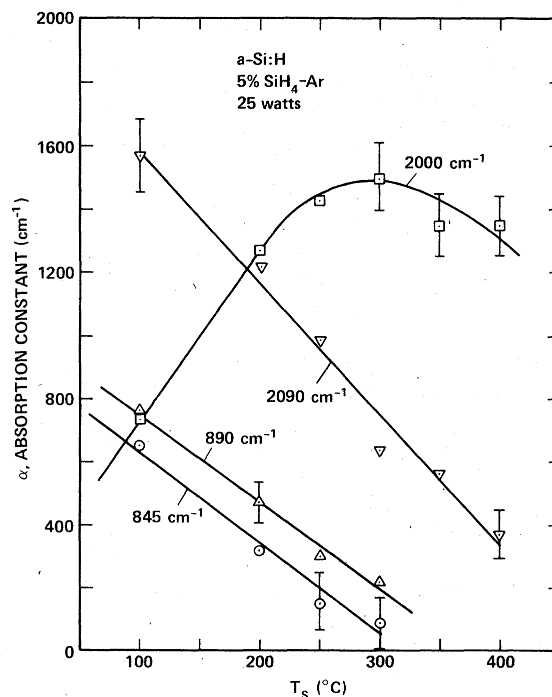


FIG. 4. Absorption constants for $a$-Si:H as a function of $T_s$ for anode samples.

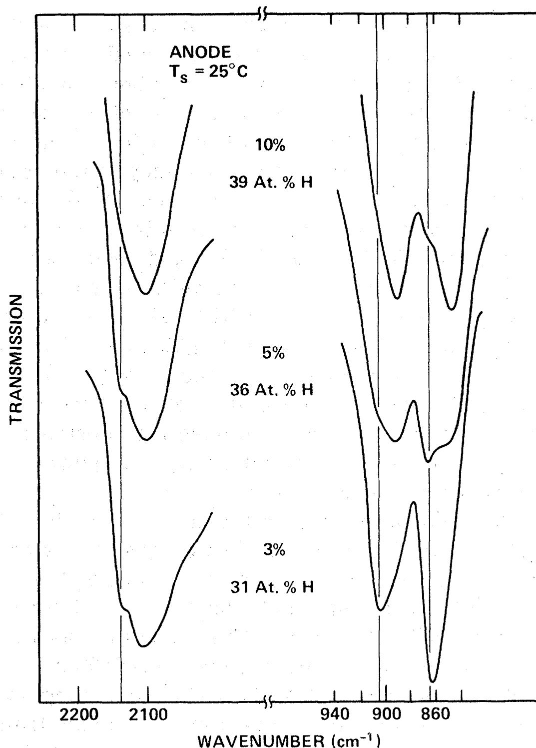


FIG. 5. ir transmission of $a$-Si:H for $T_s$ = 25 °C. The relative dilution of $SiH_4$ in Ar is given as is the atomic percent of hydrogen.

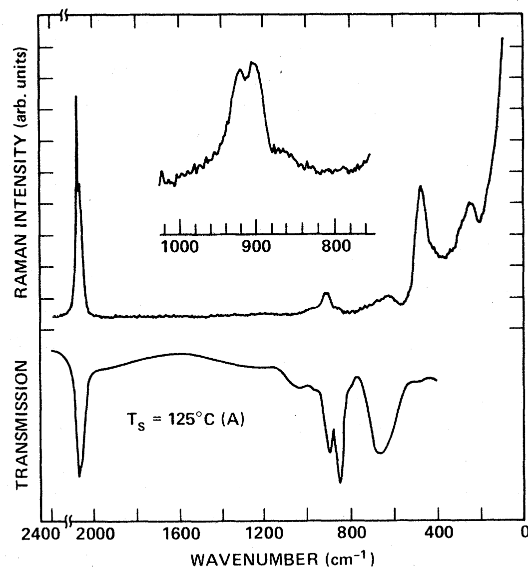


FIG. 6. ir transmission and Raman spectrum of $a$-Si:H for $T_s$ = − 125 °C. The inset is an expansion of the Raman spectrum in the 800–1000-cm$^{-1}$ frequency range. (A) indicates that the sample was produced on an anode substrate.

950-cm$^{-1}$ regime; a lower-frequency doublet at 845 cm$^{-1}$, 890 cm$^{-1}$ and a higher-frequency doublet at 862 cm$^{-1}$, 907 cm$^{-1}$. The absorption at 2140 cm$^{-1}$ is correlated with the absorption of the higher-frequency doublet. Note further that the frequency of the maximum bond-stretching absorption in these room-temperature samples is at 2100 cm$^{-1}$, about 10 cm$^{-1}$ higher in frequency than the corresponding feature of the samples produced on the higher-temperature (230 °C) substrates. Studies of the ir absorption on samples produced at intermediate substrate temperatures indicate a continuous shift in the position of this maximum in the absorption between about 2080 and 2100 cm$^{-1}$.

The ir absorption and Raman scattering from a sample produced on a low-temperature substrate, $T_s$ = −125 °C are shown in Fig. 6. Note first that the dominant ir absorption and Raman scattering in the bond-stretching regime is at ~2140 cm$^{-1}$ with a weaker feature at ~2100 cm$^{-1}$. The ir absorption in the bond-bending regime is dominated by the higher-frequency doublet, 862, 907 cm$^{-1}$; however, there is also evidence of the lower-frequency doublet at 845,890 cm$^{-1}$. The Raman spectrum displays two features near 900 cm$^{-1}$; one of these is at 905 cm$^{-1}$ and correlates with one component of the bond-bending doublet as observed in the ir absorption. The second component is at 920 cm$^{-1}$ and correlates with a shoulder in the ir absorption. There is only very weak Raman scattering between 840 and 860 cm$^{-1}$ that can be correlated with the lower frequency component of either doublet. Additional features in the Raman spectrum below about 500 cm$^{-1}$ are due to Si-Si vibrations, and the broad continuum between 500 and 1000 cm$^{-1}$ is due to second-order scattering.[5] The ir absorption shows additional features between 1000 and 1200 cm$^{-1}$. These are due to oxidation. The behavior of these absorptions with time establishes that the oxidation occurs after the deposition process.

## VIBRATIONAL ANALYSIS

Consider the bonding of H to a Si site which is then connected to the network through at least one Si-Si bond. There can be either one, two, or three H atoms at such a site. In all cases, the local bonding geometry is assumed to be tetrahedral. Since the mass of H is very small compared to that of Si, $m_H/m_{Si} \sim 0.03$, the vibrational modes of interest here can be described by considering the displacements of the H atoms. The properties of these modes can be obtained from a consideration of an appropriate tetrahedral cluster; for example, the modes of an $SiH_2$ group connected to a Si network in a tetrahedral environment are obtained from the cluster $Si_2SiH_2$.[5]

The molecular clusters relevant to the three local bonding configurations, as well as schematic representations of the vibrational modes involving H motions, are displayed in Fig. 7. The vibrational modes of these H containing groups have been discussed in other publications relating to H in $a$-Si.[4,5] The modes of the corresponding C-H groups, CH, $CH_2$, and $CH_3$ have also been studied, both theoretically and experimentally.[10] One important aspect of these vibrational modes that has not been discussed with respect to Si-H, but that is well understood in the C-H groups, relates to a separation of the vibrations into modes which involve changes in the Si-H bond-length and/or the H-Si-H bond angle and modes in which the SiH, $SiH_2$, or $SiH_3$, groups rotate as a rigid unit. This separation is illustrated by considering the modes of $SiH_2$. The number of vibrational modes of such a H-containing group is simply three per H-atom; thus there are six modes for $SiH_2$. As it turns out, these are all nondegenerate. There are three modes for which the bond-length or bond-angle coordinates change; symmetric and asymmetric bond-stretching modes and a scissors-type bond-bending mode. The remaining three modes are then rotations of the $SiH_2$ group about the three coordinate axes of the tetrahedral cluster: a twisting mode about the $z$ axis, a wagging mode about the $x$ axis, and a rocking mode about the $y$ axis. In a similar way, the modes of SiH separate into one mode of the first type, a bond-stretching mode and one of the second type, a doubly degenerate bond-bending (rocking or wagging) mode with rotation about either the $x$ or $y$ axis. For the $SiH_3$ group, the modes of the first type occur as doubly degenerate and nondegenerate bond-stretching and bond-bending modes. In addition, the doubly degenerate rocking or wagging mode corresponds to a rotation of the group about either the $x$ or $y$ axis, while the nondegenerate twisting mode is a rotation about the $z$ axis.

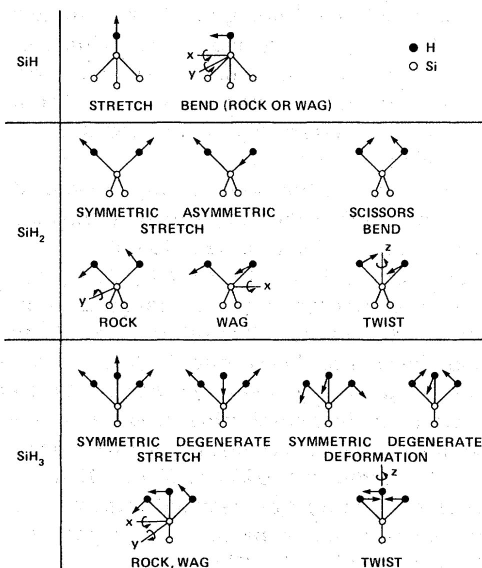


FIG. 7. Local Si-H vibrations for SiH, $SiH_2$, and $SiH_3$ groups.

The properties of these modes, their symmetry character, activity, as well as estimate frequencies are summarized in Table I. The symmetry character has been determined from the tetrahedral molecular cluster. For modes involving changes in the bond lengths and bond angles, the frequencies can be estimated using the valence forces obtained from a consideration of the vibrational modes of silane and substituted silanes.[5,11,12] The forces are adjusted for the induction effects caused by polar neighbors.[13] It is also possible to estimate the frequency of the rocking modes for SiH and $SiH_2$ using a Si-Si-H bond-bending force that is intermediate in value between that of H-Si-H and Si-Si-Si.[5] When extended to $SiH_3$, this calculation yields a rocking mode frequency of 505 $cm^{-1}$, which we now believe is not a good estimate. The frequencies of the rocking modes of $SiH_3$ and the twisting and wagging modes of $SiH_2$ and $SiH_3$ can be better estimated from the frequencies of the isostructral $CH_2$ and $CH_3$ groups. Alternatively, a calculation of these frequencies requires an extension of the force field to include torsional forces.

Interactions between H atoms on different Si sites can also produce multiplet features in the spectra. These interactions can be of two kinds, those that occur through the Si atoms, as between $SiH_2$ groups in a polysilanelike chain segment, or direct interactions between H atoms bonded to different Si atoms. Interactions of both types produce relattively small splittings in the modes of the basic groups, ~10 $cm^{-1}$.[14,15] Changes in the optical activity of a vibrational mode can also be brought about by changes in the symmetry associated with H groups on nearest-neighbor Si sites. For example, all of the modes of the $SiH_2$ group become both ir and Raman active in an infinite-chain configuration, $(SiH_2)_\infty$.

## DISCUSSION

Whereas there is agreement concerning the spectral features attributed to an SiH group (i.e., the absorption bands at 2000 and 630 $cm^{-1}$), there are at least two different structural models for the interpretation of spectra which display the bond-bending signatures in the 800–950-$cm^{-1}$ regime

TABLE I. Si-H vibrations for SiH, $SiH_2$, and $SiH_3$. Included in the table are the local symmetry, the character of the vibrational mode, its symmetry and activity, and an estimated frequency. The superscripts $P$ and $D$ refer, respectively, to polarized and depolarized Raman scattering. $I$ indicates an inactive mode.

| Structural group (local symmetry) | Mode | Symmetry | Activity | Estimated frequency ($cm^{-1}$) |
|---|---|---|---|---|
| SiH | Stretch | $A_1$ | ir, $R^P$ | 2000 |
| ($C_{3v}$) | Bend | $E$ | ir | 650 |
| $SiH_2$ | Symmetric stretch | $A_1$ | ir, $R^P$ | 2100 |
| ($C_{2v}$) | Asymmetric stretch | $B_1$ | ir, $R^D$ | 2100 |
| | Bend-scissors | $A_1$ | ir, $R^P$ | 900 |
| | Wag | $B_2$ | ir, $R^D$ | 850 |
| | Twist | $A_2$ | $R^D$ | 820 |
| | Rock | $B_1$ | ir, $R^D$ | 650 |
| $SiH_3$ | Symmetric stretch | $A_1$ | ir, $R^P$ | 2150 |
| ($C_{3v}$) | Asymmetric stretch | $E$ | ir, $R^D$ | 2150 |
| | Degenerate deformation | $A_1$ | ir, $R^P$ | 900 |
| | Symmetric deformation | $E$ | ir, $R^D$ | 850 |
| | Wag, rock | $E$ | ir, $R^D$ | 630 |
| | Twist [a] | $A_2$ | $I$ | 500 |

[a] This is not a mode of an Si-$SiH_3$ molecular cluster. The symmetry assignment is derived from a consideration of a larger cluster, $Si_4$-$SiH_3$, with $C_{3v}$ symmetry.

and therefore contain $SiH_2$ and/or $SiH_3$ groups.[4,5] Table II summarizes our assignments of the Si-H vibration in terms of four local atomic environments, SiH, $SiH_2$, $(SiH_2)_n$, and $SiH_3$. As we have already noted, the incidence of absorption in the bond-bending frequency regime is accompanied by additional bond-stretching absorptions at 2090 and 2140 $cm^{-1}$. On the basis of their studies, BCC concluded that the bond-stretching absorptions at 2000, 2090, and 2120 $cm^{-1}$ (we find this absorption at 2140 $cm^{-1}$) were due, respectively, to SiH, $SiH_2$, and $SiH_3$ groups. They also concluded that the symmetric stretching mode of the $SiH_3$ group was at 2090 $cm^{-1}$. BCC assigned the bond-bending feature at 890 $cm^{-1}$ (880–895 $cm^{-1}$) to both $SiH_2$ and $SiH_3$, specifically to the scissors mode of $SiH_2$ and the degenerate deformation of $SiH_3$. The mode at 850 $cm^{-1}$ (835–855 $cm^{-1}$) was assigned to the symmetric deformation of $SiH_3$. KLN emphasized the bond-bending modes and indicated that the doublet feature could be also interpreted in terms of interacting $SiH_2$ groups, with the high-frequency component at ~890 $cm^{-1}$ being the scissors mode of an isolated $SiH_2$ group, the same assignment as BCC, and the low-frequency component at 845 $cm^{-1}$ being due to a mode associated with nearby $SiH_2$ groups. For example, they pointed out that this mode at 845 $cm^{-1}$ could be an $SiH_2$ wagging vibration made active through a change in local symmetry associated with the $(SiH_2)_n$ configuration.[5]

TABLE II. Assignments for the principal ir and Raman features in a-Si:H as a function of the local structural groups, SiH, $SiH_2$, $(SiH_2)_n$, and $SiH_3$.

| Group | Frequency ($cm^{-1}$) | Assignment |
|---|---|---|
| SiH | 2000 | Stretch |
| | 630 | Bend |
| $SiH_2$ | 2090 | Stretch |
| | 880 | Bend-scissors |
| | 630 | Rock |
| $(SiH_2)_n$ | 2090–2100 | Stretch |
| | 890 | Bend-scissors |
| | 845 | Wag |
| | 630 | Rock |
| $SiH_3$ | 2140 | Stretch |
| | 907 | Degenerate deformation |
| | 862 | Symmetric deformation |
| | 630 | Rock |

Consider first the bond-stretching modes. It is well established that the vibrational frequencies of Si-H stretching modes of a substituted silane (e.g., $SiHR_1R_2R_3$, where $R_i$ = F, Cl, Br, $CH_3$, $C_2H_5$, $C_5H_6$, etc.) can be shifted by relatively large amounts by changing the nature of the other three atoms or groups bonded to the Si atom.[13] The vibrational frequency of the SiH group increases as the electronegativity of the substituting group increases. For example, the SiH frequency is 2314.5 $cm^{-1}$ in $SiHF_3$ and reduced to 2234 $cm^{-1}$ in $SiHBr_3$.[11] This frequency is further reduced when the halogen atoms are replaced by organic groups, such as $CH_3$, $C_2H_5$, and $C_5H_6$. The range of SiH vibrational frequencies in substituted silanes is from approximately 2100 to 2325 $cm^{-1}$.[11] It has been shown that the frequency of the SiH vibration

scales with the sum of the electronegativities of these atoms or groups.[13] Specifically we can write

$$v(\mathrm{SiH}) = a \sum x_i(R_i) + m \ , \quad (1)$$

where $a$ and $m$ are empirically determined constants and where $x_i$ is the electronegativity of the $R_i$ group in a molecule of the form $SiHR_1R_2R_3$. This relationship can be extended to include $SiH_2$ and $SiH_3$ vibrations. Figure 8 displays plots of vibrational frequency versus electronegativity for a number of substituted silanes. We have used the stability-ratio (SR) electronegativity scale since it affords a convenient way of obtaining the electronegativity of organic groups such as $CH_3$.[16] (Note that the SR scale maps onto the more commonly used Pauling scale.) The solid lines in the figure are a least-squares fit to the data points. The uncertainty in the predicted value of $v$ for a given $\sum x_i(R_i)$ is also indicated. The open circles represent the assignments for the stretching vibrations of SiH, $SiH_2$, and $SiH_3$ groups in $a$-Si:H alloys. These are the same as those proposed by BCC, except for the symmetric mode of the $SiH_3$ group. Alternatively, the assignments can be made by considering the three characteristic stretching frequencies and the appropriate values for $\sum x_i(R_i)$, and then matching the points to the appropriate straight lines. Note that the vibrational frequencies for all three types of SiH vibrations lie well below the corresponding frequencies in substituted silanes. This is a direct result of the lower electronegativity of Si as compared to the halogen or organic groups. The values of $\sum x_i(R_i)$ used in this comparison are for the

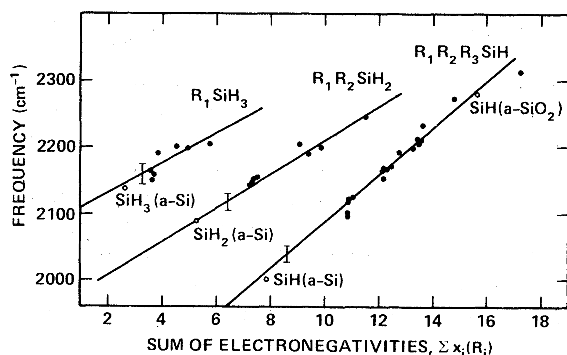


FIG. 8. Frequency of Si-H stretching vibrations as function of the electronegativity of the atoms or groups bonded to the Si atom. The solid points are for substituted silane molecules. The line represents a linear fit to these points. The error bar indicates the standard deviation. The open circles are the frequencies of Si-H vibrations in the $a$-Si:H alloys and in $SiO_2$.

next neighbor Si atoms, three Si atoms for SiH, two for $SiH_2$, and one for $SiH_3$. This represents an approximation since these next neighbor Si atoms are in turn bonded to other atoms in the network structure.[17] However, calculations demonstrate that the electronic properties of the Si-H bond, which ultimately establish that the vibrational frequencies are highly local, so that effects from more distant neighbors may be neglected. This consideration is also born out in model calculations for the vibrational modes[5] which have established a similar local nature. These calculations, as well as comparisons with various silane molecules, indicate very small splittings, $< 10$ cm$^{-1}$, between the symmetric and asymmetric stretching modes. Our comparisons of ir absorption and Raman scattering lead to a similar conclusion. Hence we assign the 2090-cm$^{-1}$ feature to vibrations of the $SiH_2$ group. BCC assigned this frequency to the symmetric stretching mode of $SiH_3$ as well as to $SiH_2$ vibrations. Our ir and Raman data for the $T_S = -125$ °C substrate indicate that the two stretching modes of $SiH_3$ are at approximately 2140 cm$^{-1}$.

We now consider the implications of the bond-stretching frequency assignments for the bond-bending modes in the 800–950-cm$^{-1}$ regime. The correlation between the absorption bands at 2090 and 890 cm$^{-1}$ establishes the 890-cm$^{-1}$ absorption as the scissors mode of the $SiH_2$ group in agreement with the previous assignments of BCC and KLN. Since the 845-cm$^{-1}$ doublet component occurs in samples which have absorption at 2090 cm$^{-1}$, but not at 2140 cm$^{-1}$, it is also associated with the $SiH_2$ group. Two assignments are then possible. The first is that it is an additional scissors mode split off in frequency by coupling between H atoms on neighboring $SiH_2$. Studies of crystalline polyethylene[14,15] indicate that H...H forces can promote such a splitting of the bond-bending mode with both components displaying ir activity. However, the sharpness of the 845-cm$^{-1}$ component of the doublet speaks against this coupling mechanism. Analysis of the vibrational spectra of a number of organic molecular crystals indicates that the H...H forces vary significantly with the interatomic spacing[14,15] so that in an amorphous solid one would not expect a sharp mode indicative of a single characteristic H...H spacing. An alternative explanation for the 845-cm$^{-1}$ mode is suggested by comparisons with the ir-absorption spectrum of plasma polymerized polyethylene.[18,19] These materials display a doublet structure in the bond-bending frequency regime. The higher-frequency component at 1450 cm$^{-1}$ is assigned to the $CH_2$ scissors mode, and the lower-frequency component at 1365 cm$^{-1}$ is

thought to be a bond wagging mode of $CH_2$.[19] This assignment of the wagging mode is supported by theoretical calculations and by experiments on long chain alkanes in which an additional very sharp feature at 1377 $cm^{-1}$, attributed to the symmetric deformation of $CH_3$ groups, can be identified through scaling arguments.[20] That is, the ratio of $CH_3$ to $CH_2$ groups can be varied in order to confirm the structural assignments for these two vibrations with nearly equal frequencies. Comparisons between "normal" and plasma polymerized polyethylene indicate a significant increase in the ir-activity of this 1365-$cm^{-1}$ mode in the plasma polymerized material. This suggests an analagous interpretation for the development of the 845-$cm^{-1}$ feature in the $a$-Si:H alloys. The mode is the wagging mode of the $SiH_2$ group, which is at best weakly ir active for an isolated $SiH_2$ group. The ir strength of the mode increases as a result of the presence of neighboring $SiH_2$ groups. This change in activity is related to a change in the local symmetry which increases the ir activity of the wagging vibration over that of an isolated $SiH_2$ group. This model then explains the presence of the 845-$cm^{-1}$ vibration in samples containing the $SiH_2$ 2090-$cm^{-1}$ bond-stretching vibration. It also provides an explanation for the scaling relationships between the absorption bands at 845 $cm^{-1}$ and 890 $cm^{-1}$ (see Fig. 3). Specifically, all $SiH_2$ groups contribute to the relatively strong absorptions at 890 and 2090 $cm^{-1}$, whereas only near-neighbor pairs of $SiH_2$ groups [or perhaps larger chain segments, $(SiH_2)_n$] contribute to a strong absorption at 845 $cm^{-1}$. Isolated $SiH_2$ groups are assumed to yield weak ir absorption at 845 $cm^{-1}$. The cathode samples, produced on 230 °C substrates, contain isolated $SiH_2$ groups, while the anode samples display an increased $(SiH_2)_n$ incorporation as the rf power is raised. Studies of the vibrational spectra of cyclopentasilane, $Si_5H_{10}$, by ir and Raman spectroscopy[21] also indicate more than one mode in the "bond-bending" frequency regime, 850–950 $cm^{-1}$. This molecule contains only $SiH_2$ units, so that this multiplicity of modes also indicates optical activity in a bond-wagging mode that is promoted by a coupling of the $SiH_2$ groups through the ring structure. Similar spectral assignments have been proposed for the $CH_2$ scissors and wagging modes in cyclohexane, $C_6H_{12}$.[22]

As discussed earlier, a correlation between the absorption strength at 2140 $cm^{-1}$ and the doublet mode at 862, 907 $cm^{-1}$ was also established (see Fig. 5). The 2140-$cm^{-1}$ mode is assigned to $SiH_3$, so that the doublet components are then the deformation modes of the $SiH_3$ group. The higher-frequency component is the degenerate deformation mode, and the lower-frequency component is the symmetric deformation mode. The multiplicity of bond-bending modes in the 5% dilution room-temperature sample then implies both $(SiH_2)_n$ and $SiH_3$ groups. Similar considerations apply for the low-temperature samples. It should, however, be noted that in the room-temperature samples, the relative abundance of the $SiH_3$ groups is not simply related to the amount of incorporated H.

The interpretation of the Raman spectra of the low-temperature sample can now be made based on these assignments (see Fig. 6). The Raman response at 905 $cm^{-1}$ must have a contribution from the degenerate deformation mode of $SiH_3$ (the higher-frequency component at 907 $cm^{-1}$). The absence of comparable strength Raman scattering between 840 and 860 $cm^{-1}$ implies weaker Raman activity in the symmetric bending mode of the $SiH_3$ group and the wagging mode of $SiH_2$. This observation is supported by comparisons with the Raman response of disilane, $Si_2H_6$,[23] and other molecules containing $SiH_3$ groups, which also indicate very weak Raman response for the symmetric deformation of $SiH_3$. The mode at 920 $cm^{-1}$ in the Raman scattering is also believed to be associated with the $SiH_3$ groups; however, it does not appear as a separate feature in the ir spectrum but, rather, contributes to a shoulder on the higher frequency doublet component.

It is not possible to provide an independent check of the $SiH_2$-$SiH_3$ bending-mode assignments using silane polymer chemistry. However, there is very strong support to be dervied from hydrocarbon chemistry, specifically from ir and Raman studies of polypropylene.[24,25] The polymer repeat unit of polypropylene has both $CH_2$ and $CH_3$ groups. The contributions of these groups to the ir absorption can be separated by selective deuteration;[24] this is illustrated in Fig. 1 of Ref. 24. Samples containing no deuterium exhibit two pairs of doublets in the bond-bending frequency regime (1350–1475 $cm^{-1}$). Deuteration of the $CH_2$ and CH groups establishes that the higher-frequency doublet is due to the $CH_3$ group. A study of the Raman spectrum[25] of polypropylene indicates a similar activity for the bond-bending modes of the $CH_3$ groups. There is strong scattering at 1475 $cm^{-1}$, the frequency of the degenerate deformation, and virtually no scattering at 1375 $cm^{-1}$ at the frequency of the symmetric deformation.

Another outgrowth of our present study relates to the vibrational properties of $a$-Ge:H alloys. Previously, Connell and Pawlik[26] (CP) identified two ir-absorption bands of $a$-Ge:H in the bond-stretching frequency range; one at 1855 $cm^{-1}$

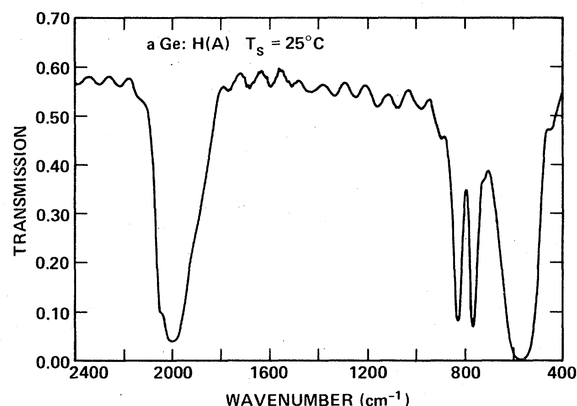


FIG. 9. The ir transmission of $a$-Ge:H for $T_S = 25$ °C. (A) indicates that the sample was produced on an anode substrate.

(0.23 eV) and the second at 1976 $cm^{-1}$ (0.245 eV). They assigned both bands to a GeH group, the absorption at 1976 $cm^{-1}$ being associated with GeH bonds in the bulk, and the 1855 $cm^{-1}$ absorption with GeH groups on the surface of a void. The absense of detectable absorption in the 750–850-$cm^{-1}$ regime was used by them as an argument against the presence of $GeH_2$ or $GeH_3$ groups. The films studied by CP were produced by sputtering Ge in a H ambient. We have produced alloys of $a$-Ge:H by the plasma decomposition of $GeH_4$ (germane) and display the ir absorption of a sample produced on a room-temperature substrate in Fig. 9. These absorption spectra are qualitatively similar to those produced by the plasma decomposition of $SiH_4$ for the same set of deposition parameters. For example, the spectrum of the $a$-Ge:H sample in Fig. 9 is similar to the corresponding $a$-Si:H spectrum in Fig. 6, but with each spectral feature shifted to a lower frequency by approximately 100 $cm^{-1}$. On the basis of this comparison, we assign the shoulder at 2050 $cm^{-1}$ to a bond-stretching vibration of $GeH_3$, and the broad absorption at 1980 $cm^{-1}$ to $GeH_2$. The doublet at 770 $cm^{-1}$, 830 has contributions from both $GeH_2$ and $GeH_3$ groups. Our studies suggest that the absorption reported at 1976 $cm^{-1}$ by CP is associated with $GeH_2$ rather than GeH.

Finally, from the analysis presented above, the characteristics of Si-H vibrations in hydrogen-containing Si-O alloys can be explored. Included in Fig. 8 is the experimentally determined frequency for the Si-H vibration in $SiO_2$.[27] This falls within a standard deviation of the fit line and provides a further demonstration of applicability of this analysis to network solids. The relationships shown in Fig. 8 can then be used to estimate the Si-H bond-stretching frequencies in partially oxidized $a$-Si:H alloys. For example, in material produced both by adding oxygen to the gas during preparation or by exposure to the ambient, studies performed in our laboratory, and by Paesler *et al*.[28] indicate no observable absorption due to OH groups, but additional absorptions between 900 and 1100 $cm^{-1}$ and in the 2100–2250-$cm^{-1}$ regime. The absorptions between 900 and 1100 $cm^{-1}$ are due to Si-O vibrations, whereas those between 2100 and 2250 $cm^{-1}$ are due to SiH vibrations in which the Si atom is bonded to one or more O atoms. For example, the Si-H vibrational frequency will be pulled to 2100 $cm^{-1}$ if there is one O in the local cluster, and to 2185 $cm^{-1}$ if there are two O atoms. Similarly, the stretching mode of an $SiH_2$ group will be shifted to a frequency of about 2160 $cm^{-1}$ if there is one O atom bonded to the Si.

## CONCLUSION

The experimental results reported in this paper have enabled us to separate the contributions of SiH, $SiH_2$, and $SiH_3$ groups and to demonstrate that neighboring $SiH_2$ groups, $(SiH_2)_n$, as well as $SiH_3$ can produce a doublet structure in the bond-bending frequency regime. Our analysis therefore reconciles the previously proposed structural interpretations of both BCC and KLN, and adds an additional degree of refinement. Through the establishment of correlations between the bond-stretching modes at 2090 and 2140 $cm^{-1}$ and the two pairs of doublets, 845, 890 $cm^{-1}$ and 862, 907 $cm^{-1}$, respectively, we have been able to separate the contributions due to $SiH_2$ and $SiH_3$ groups. Samples produced by plasma decomposition of $SiH_4$ onto high temperature substrates ($T_S > 200$ °C) have local environments containing SiH groups, $SiH_2$ groups, and $(SiH_2)_n$ groups. Samples produced at room temperature and below display features that can be attributed to $SiH_3$ groups as well as $(SiH_2)_n$. For the range of deposition parameters explored in this study, the $SiH_3$ groups become increasingly important as the substrate temperature is decreased.

*Note added in proof.* Recently the Harvard group has prepared a film of $a$-Ge:H by sputtering containing 12–13 at.% H.[29] The films studied by Connell and Pawlik[26] contained at most 8 at.% H. The film containing 12–13 at.% H shows a relatively weak absorption at about 820 $cm^{-1}$, which is here attributed to the scissors-bending mode of the $GeH_2$ group. This film also displays bond-stretching absorptions near 1855 and 1976 $cm^{-1}$; however,

the relative absorption at 820 $cm^{-1}$ is considerably weaker than the doublet absorption (770 $cm^{-1}$, 830 $cm^{-1}$) shown in Fig. 9. A possible explanation for these differences in the relative absorption is that the feature in the sputtered *a*-Ge:H film is due to an isolated $GeH_2$ group, whereas, the doublet in Fig. 9 clearly has contributions from near-neighbor $GeH_2$ and $GeH_3$ groups.

---

[1]A. J. Lewis, G. A. N. Connell, W. Paul, J. R. Pawlik, and R. J. Temkin, in *Tetrahedrally Bonded Amorphous Semiconductors*, edited by M. H. Brodsky and S. Kirkpatrick (Am. Inst. Phys., New York, 1974), p. 27.

[2]J. I. Pankove, M. A. Lampert, and M. L. Tarng, Appl. Phys. Lett. 32, 439 (1978); J. I. Pankove, Appl. Phys. Lett. 32, 812 (1978).

[3]J. C. Knights, G. Lucovsky, and R. J. Nemanich, J. Non-Cryst. Solids (to be published).

[4]M. H. Brodsky, M. Cardona, and J. J. Cuomo, Phys. Rev. B 16, 3556 (1977).

[5]J. C. Knights, G. Lucovsky, and R. J. Nemanich, Philos. Mag. B 37, 467 (1978).

[6]C. C. Tsai, H. Fritzsche, M. H. Tanielian, P. J. Gaczi, P. D. Persans, and M. A. Vesaghi, in *Amorphous and Liquid Semiconductors*, edited by W. E. Spear (Centre for Industrial Consultancy and Liaison, Univ. of Edinburgh, 1978), p. 339.

[7]E. C. Freeman and W. Paul, Phys. Rev. B 18, 4288 (1978).

[8]J. C. Knights, in *Structure and Excitations of Amorphous Solids*, edited by G. Lucovsky and F. L. Galeener (Am. Inst. of Phys., New York, 1976), p. 296; Phil. Mag. 34, 663 (1976).

[9]R. A. Street, J. C. Knights, and D. K. Biegelsen, Phys. Rev. B 18, 1880 (1978).

[10]L. J. Bellamy, *The Infra-red Spectra of Complex Molecules* (Chapman and Hall, London, 1975); R. Zbinden, *Infrared Spectroscopy of High Polymers* (Academic, New York, 1964).

[11]G. J. Janz and Y. Mikawa, Bull. Chem. Soc. Jpn. 34, 1495 (1961).

[12]C. W. F. T. Pistorius, J. Chem. Phys. 27, 965 (1957).

[13]A. L. Smith and N. C. Angelotti, Spectrochim. Acta 15, 412 (1959).

[14]R. G. Snyder, J. Mol. Spectros. 7, 116 (1961).

[15]M. Tasumi and S. Krim, J. Chem. Phys. 46, 755 (1967).

[16]R. T. Sanderson, *Chemical Periodicity* (Reinhold, New York, 1960).

[17]G. Lucovsky, Solid State Commun. (to be published).

[18]L. F. Thompson and K. G. Mayham, J. Appl. Polym. Sci. 16, 2291 (1972).

[19]H. Kobayashi, A. T. Bell, and M. Shen, J. Appl. Polym. Sci. 17, 885 (1973).

[20]C. Janford, *Physical Chemistry of Macromolecules* (Wiley, New York, 1961), p. 83.

[21]E. Hengge and G. Bauer, Angew. Chem. Internat. 12, 316 (1973).

[22]R. G. Snyder and J. H. Schachtschneider, Spectrochim. Acta 21, 169 (1965).

[23]G. W. Bethke and M. K. Wilson, J. Chem. Phys. 26, 1107 (1957).

[24]H. Tadakoro, M. Kobayashi, M. Ukita, K. Yasufuku, and S. Murahashi, J. Chem. Phys. 42, 1432 (1965).

[25]R. F. Schaufele, J. Opt. Soc. Am. 57, 105 (1967).

[26]G. A. N. Connell and J. R. Pawlik, Phys. Rev. B 13, 787 (1976).

[27]F. L. Galeener and R. H. Geils, in *The Structure of Non-Crystalline Materials*, edited by P. H. Gaskell (Taylor and Francis, London, 1977), p. 223.

[28]M. A. Paesler, D. A. Anderson, E. C. Freeman, G. Moddel, and W. Paul, Phys. Rev. Lett. 41, 1492 (1978).

[29]S. Oguz and M. A. Paesler, Bull. Am. Phys. Soc. 23, 247 (1978).